

¹ Drought indices of water demand and supply, soil moisture, vegetation, and
² its impact on LULCC in continental Chile

³ Francisco Zambrano^{a,1,*}

^a Universidad Mayor, Hémera Centro de Observación de la Tierra, Facultad de Ciencias, Escuela de Ingeniería en Medio Ambiente y Sustentabilidad, Santiago, Chile, 7500994

⁴ **Abstract**

Human-induced greenhouse gas emissions have increased the frequency and/or intensity of weather and climate extremes. Central Chile has been affected by a persistent drought which is impacting the hydrological system and vegetation development. The region has been the focus of research studies due to the diminishing water supply, this persistent period of water scarcity has been defined as a “mega drought”. Nevertheless, our results evidence that the water deficit has expanded beyond. Our goal is to analyze the impact of drought, measured by drought indices of water supply/demand and vegetation status, in the LULCC (land use land cover change) over continental Chile. For the analysis, continental Chile was divided into five zones according to a latitudinal gradient: “Norte Grande”, “Norte Chico”, “Zona Central”, “Zona Sur”, and “Zona Austral”. We used monthly climatic re-analysis variables for precipitation, temperature and soil moisture for 1981-2023 from ERA5-Land; and MODIS (Moderate-Resolution Imaging Spectroradiometer) product MCD12Q1 for land cover for 2001-2021, and the NDVI vegetation index from product MOD13A2 collection 6.1 for 2000-2023, both from collection 6.1. We estimated atmospheric evaporative demand (AED) by combining the Hargreaves-Samani equation with the ERA5-Land temperature. We derived the drought indices SPI (Standardized Precipitation Index), SPEI (Standardized Precipitation Evapotranspiration Index), EDDI (Evaporative Demand Drought Index), zcSM (standardized anomaly of cumulative soil moisture), and the zcNDVI (standardized anomaly of cumulative NDVI). These indices were calculated for time scales of 1, 3, 6, 12, 24, and 36 months, except for zcNDVI (1, 3, and 6 months). We analyzed the temporal correlation of SPI, SPEI, EDDI, and zcSM with zcNDVI to have insights into the impact of water supply and demand on vegetation. Our results showed that LULCC had an increasing trend of 412 [km²yr⁻¹] of forest expansion in the “Zona Sur”, together with a decreasing trend of 24 [km²yr⁻¹] of cropland contraction in the “Zona Central” meanwhile the “Zona Sur” showed an increase of 31 [km²yr⁻¹], and a contraction of 80 [km²yr⁻¹] of bare soil in the “Zona Austral”. The EDDI was the less correlated index for the five macro zones and the five types of land cover, showing that the temperature in Chile has little impact on vegetation. Higher r-squared values, between 0.5 and 0.8, were obtained at “Norte Chico” and “Zona Central” for the land cover types of savanna, shrubland, grassland, and croplands for the indices SPEI and zcSM at time scales of 12 and 24 months. The forest type reaches a r-squared of ~0.5 for zcSM of 12 months. The results indicate that the “Norte Chico” and “Zona Central” are the most sensitive regions to water supply deficits longer than a year, potentially explained by a low capacity of water storage in those zones that should be further investigated.

⁵ **Keywords:** drought, land cover change, satellite

*Corresponding author

Email address: francisco.zambrano@umayor.cl (Francisco Zambrano)

¹This is the first author footnote.

6 **1. Introduction**

7 The sixth assessment report (AR6) of the IPCC [1] indicates that human-induced greenhouse gas emissions
8 have increased the frequency and/or intensity of some weather and climate extremes, and the evidence has
9 been strengthened since AR5 [2]. There is high confidence that increasing global warming can expand the
10 land area affected by increasing drought frequency and severity [3]. Furthermore, drought increases tree
11 mortality and triggers changes in land cover and, consequently, land use, thus impacting ecosystems [4].
12 Nevertheless, there is a lack of understanding of how the alteration in water supply and demand is affecting
13 land cover transformations.

14 Precipitation is the primary driver of drought and is intensified by temperature [5]. Drought impacts soil
15 moisture, hydrological regimes, and vegetation productivity. Initially, drought was commonly classified as
16 meteorological, hydrological, and agricultural [6]. Lately, [7] and [8] have given an updated definition of
17 drought for the Anthropocene, suggesting that it should be considered the feedback of humans' decisions
18 and activities that drives the anthropogenic drought. Even though it has been argued that those definitions
19 do not fully address the ecological dimensions of drought. [4] proposed the ecological drought definition as
20 "*an episodic deficit in water availability that drives ecosystems beyond thresholds of vulnerability, impacts*
21 *ecosystem services, and triggers feedback in natural and/or human systems*". Moreover, many ecological
22 studies have misinterpreted how to characterize drought, for example, sometimes considering "dry" conditions
23 as "drought" [9]. On the other hand, the AR6 [1] states that even if global warming is stabilized at
24 1.5°–2°C, many parts of the world will be impacted by more severe agricultural and ecological droughts.
25 Then, there is a challenge in conducting drought research, especially to evaluate its impact on ecosystems.

26 Chile has been facing a persistent rainfall deficit for more than a decade [10], which has impacted vegetation
27 development [11] and the hydrological system [12]. Current drought conditions have affected crop
28 productivity [13, 14], forest development [15, 16], forest fire occurrence [17], land cover change [18], water
29 supply in watersheds [19], and have had economic impacts [20]. In 2019–2020, the drought severity reached
30 an extreme condition in Central Chile (30–34°S) not seen for at least 40 years, and the evidence indicates
31 that the impact is transversal to the land cover classes of forest, grassland, and cropland [11]. The prolonged
32 lack of precipitation in Central Chile is producing changes in ecosystem dynamics that must be studied.

33 For the spatiotemporal assessment of drought impact (i.e., by water supply and demand) on land cover
34 changes, we need climatic reliable variables such as precipitation, temperature, soil moisture, land cover, and
35 vegetation status. For developing countries like Chile, the weather networks present several disadvantages,
36 such as gaps, a short history, and low-quality data. Reanalysis data, as the ERA5-Land (ERA5L) [21]
37 provides hourly climatic information (precipitation, temperature, and soil moisture) without gaps since
38 1950 with global extension. ERA5L has already been used for drought assessment using the Standardized
39 Precipitation-Evapotranspiration Index (SPEI) [22] and for flash drought [23] by analyzing soil moisture
40 and evapotranspiration. On the other hand, satellite remote sensing [24, 25] is the primary method to
41 evaluate how drought impacts vegetation dynamics. Vegetation drought indices (VDI) are commonly used
42 as proxies of productivity [26, 27], which can be derived from the MODIS (Moderate-Resolution Imaging
43 Spectroradiometer). Besides, land use and land cover (LULC) change can be driven by drought [28, 29]. To
44 analyze these changes, multiple LULC products exist [30], one of those that provides time series since 2001
45 is the MCD12Q1 [31] from MODIS. The variation in water supply and demand is finally reflected in the
46 total water storage (TWS). The TWS can be retrieved by the Gravity Recovery and Climate Experiment
47 (GRACE), which allows analyzing water availability changes at coarse resolution [32, 33]. We can use climatic
48 reanalysis (ERA5L) and vegetation data (MODIS) to derive drought indices of supply (i.e., precipitation)
49 and demand (i.e., temperature) and thus evaluate the impact of drought on LULC changes. Further, the
50 TWS can be assessed with regard to the changes in water supply and demand to gain insight into the impact
51 on water storage.

52 To evaluate meteorological drought (i.e., water supply), the World Meteorological Organization (WMO;
53 [34]) recommends the Standardized Precipitation Index (SPI; [35]), a multiscalar drought index that allows
54 to monitor precipitation deficits from short- to long-term. Following the same approach, [36] incorporates

55 into the SPI the effect of temperature through the use of potential evapotranspiration, thus proposing the
56 SPEI (Standardized Precipitation Evapotranspiration Index). Similarly, to evaluate solely the evaporative
57 demand driven by temperature, [37] and [38] came up with the Evaporative Demand Drought Index (EDDI).
58 For vegetation, in a similar manner as the SPI, SPEI and EDDI; [14] proposed the zcNDVI, a standardized
59 anomaly of the cumulative Normalized Difference Vegetation Index (NDVI), which could be accumulated
60 over the growing season or any period (e.g., months), resulting in a multiscalar drought index. For soil
61 moisture, several drought indices exist, such as the Soil Moisture Deficit Index (SDMI) a normalized index
62 [39] and the Soil Moisture Agricultural Drought Index (SMADI) [40] which is a normalized index using
63 vegetation, land surface temperature, and a vegetation condition index (VCI, [41]). From TWS, we can
64 estimate the standardized terrestrial water storage index (STI) [42], a standardized anomaly that follows
65 the methodology of the SPI, SPEI, EDDI, and zcNDVI. Thereby, we have drought indices for water supply,
66 demand, and storage, which can help to make a comprehensive assessment of drought.

67 In this research, we present the raster dataset DDS4Chl, which provides climate variables and drought
68 indices of water demand and supply and vegetation productivity for continental Chile since 1981 at a monthly
69 frequency. Those were gathered from the earth observation products ERA5-Land and MODIS. Then, we
70 used DDS4Chl to analyze the impact of drought on different types of land cover classes in continental Chile.
71 The specific objectives of the study are: i) to analyze the trend on multi-scalar drought indices for water
72 demand and supply, soil moisture, and vegetation productivity for 1981–2023/2001–2023; ii) to evaluate
73 LULC change for 2001–2021 and its relation to drought indices; iii) to analyze the relationship of a proxy of
74 vegetation productivity (zcNDVI) with drought indices of water demand and supply and soil moisture; and
75 iv) to assess if the observed changes in the drought indices are linked to TWS.

76 2. Study area

77 Continetal Chile has a diverse climate condition from north to south and east to west [43] (Figure 1), which
78 determines its great ecosystem diversity (Figure 2). The Andes Mountains are a main factor in latitudinal
79 variation [44]. To describe the climate and ecosystem of Chile, we use the Koppen-Geiger release by [45] and
80 the landcover type persistance of 80% of times for 2001–2022, from the IGBP classification scheme [31] (see
81 Section 3.5). “Norte Grande” and “Norte Chico” predominate in an arid desert climate with hot (Bwh) and
82 cold (Bwk) temperatures. At the south of “Norte Chico,” the climate changes to an arid steppe with cold
83 temperatures (Bsk). Mainly, the land is barren, with a minor surface of vegetation types such as shrubland
84 and grassland. In the zones “Centro” and the north half of “Sur,” the main climate is Mediterranean, with
85 warmer to hot summers (Csa and Csb). In “Centro,” there is a major proportion (~50%) of chilean matorral
86 (shrubland and savanna), followed by grassland (~16%), forest (8%), and croplands (5%). The south part
87 of “Centro” and the north part of “Austral” are dominated by an Oceanic climate (Cfb). Those zones are
88 high in forest and grassland. The southern part of the country has a tundra climate, and in Patagonia, it is
89 a cold semi-arid area with an extended surface of grassland.

90 3. Materials and Methods

91 3.1. Data

92 3.1.1. Earth observation data

93 For water supply and demand variabes, we used ERA5-Land [21], a reanalys dataset wich provides the
94 evolution of land variables since 1950. It has a spatial resolution of 0.1°, hourly frequency and global
95 coverage. We selected the variables for total precipitation, 2 meters temperature maximum and minimum,
96 and volumetric soil water layers between 0 and 100cm of depth (layer 1 to layer 3).

97 To derive a proxy of vegetation productivity, we used the product MOD13A3 collection 6.1 from MODIS
98 [46]. It provides vegetation indices (NDVI and EVI) at 1km of spatial resolution and monthly frequency.

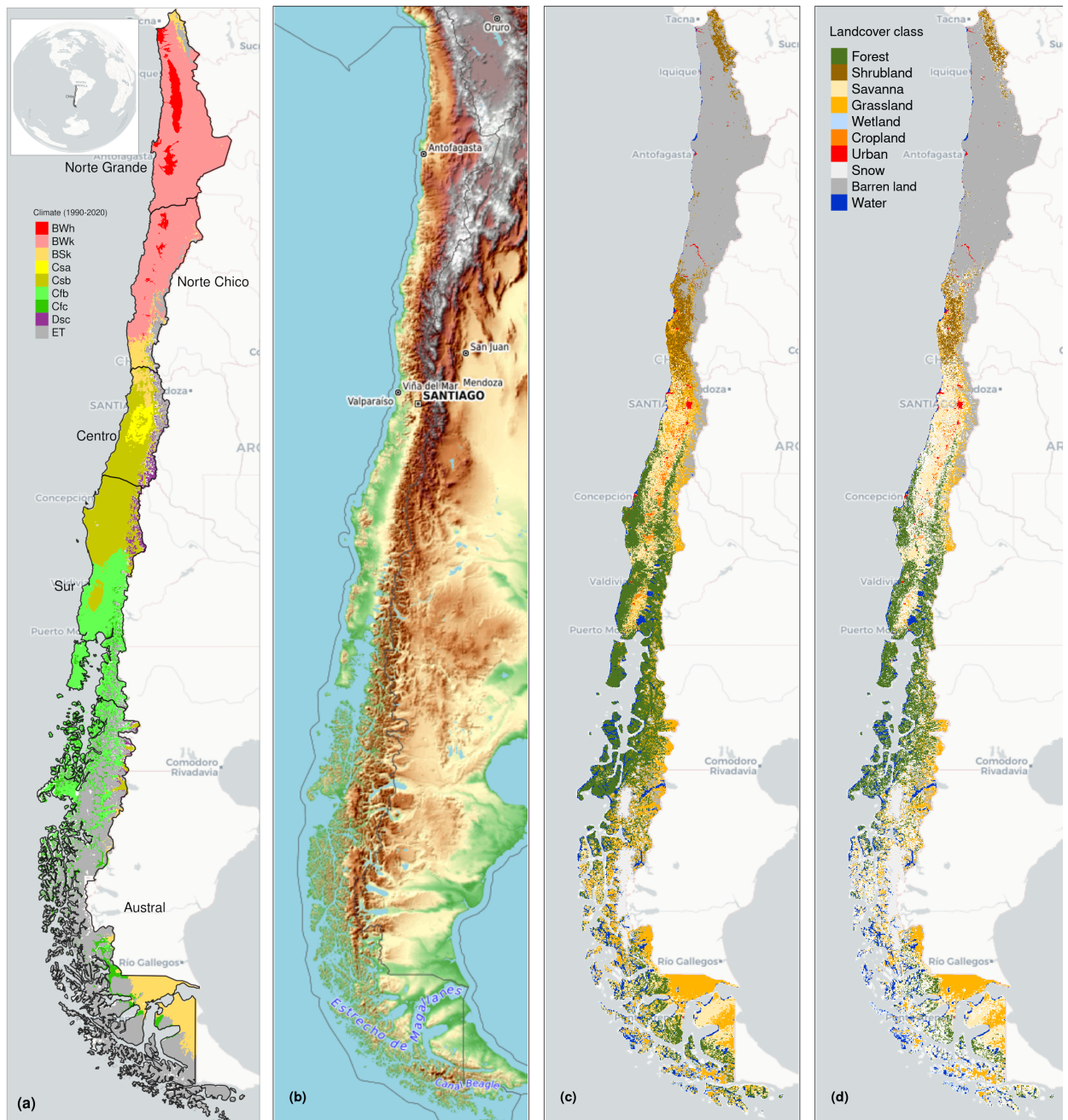


Figure 1: (a) Chile with the Koppen-Geiger climate classes and the five macrozones “Norte Grande”, “Norte Chico”, “Centro”, “Sur”, and “Austral”. (b) Topography reference map. (c) Land cover classes for 2022. (d) Persistent land cover classes (> 80%) for 2001-2022

99 3.1.2. *in-situ* data

100 3.2. Software and packages used

101 For the downloading, processing, and analysis of the spatio-temporal data, we used the open source software
 102 for statistical computing and graphics, R [47]. For downloading ERA5-Land, we used the `{ecmwfr}` package
 103 [48]. For processing raster data, we used `{terra}` [49] and `{stars}` [50]. For managing vectorial data, we

Table 1: Description of the earth observation data used

Product	Sub-product	Variable	Spatial Resolution	Period	Units	Short Name
ERA5-Land		Precipitation	0.1°	1981-2023	mm	P
		Maximum temperature			°C	T_{max}
		Minimum temperature			°C	T_{min}
		Volumetric Soil Water Content at 1m			m3/m3	SM
ERA5-Land*		Atmospheric Evaporative Demand	0.1°	1981-2023	mm	AED
	MOD13A3.061	Normalized Difference Vegetation Index			1 km	NDVI
	MCD12Q1.061	Landcover IGBP scheme			2001-2022	Landcover

*Derived from ERA5-Land with Eq. 1.

104 used `{sf}` [51]. For the calculation of AED, we used `{SPEI}` [52].

105 *3.3. Drought Indices*

106 We derived the drought indices of water supply and demand, soil moisture from the ERA5-Land dataset,
107 and vegetation from the MODIS product, all at monthly frequency.

108 For the indices EDDI and SPEI that use water demand, first we have to calculate the AED. For this, we
109 used the method of Hargreaves [53]:

$$AED = 0.0023 \cdot Ra \cdot (T + 17.8) \cdot (T_{max} - T_{min})^{0.5} \quad (1)$$

110 where Ra ($MJ m^2 day^{-1}$) is extraterrestrial radiation; T , T_{max} , and T_{min} are mean, maximum, and
111 minimum temperature ($^{\circ}C$). We calculate the centroid coordinates per pixel and use the latitude to estimate
112 Ra .

113 To evaluate water demand, we chose the *EDDI* [37, 38] index, which uses the *AED*. For supply, we used
114 the index recommended by the World Meteorological Organization (WMO) for monitoring drought, the
115 *SPI* [35]. We calculated the *SPEI*, which used a balance between P and *AED*, in this case, an auxiliary
116 variable $D = P - AED$ is used. In this study, we propose the *zcSM* (standardized anomaly of accumulated
117 soil moisture at 1 m), which uses *SM*. Finally, for the proxy of productivity, *zcNDVI*, we used the *NDVI*.
118 Before using the *NDVI*, it was smoothed following the procedure described in [14] and [13].

119 All the indices are multi-scalar and were calculated for time scales of 1, 3, 6, 12, 24, and 36 months, except
120 for *zcNDVI*, which was calculated for 6 months. The goal is to be able to evaluate short- and long-term
121 droughts in water demand and supply and soil moisture. This is particularly important for central Chile
122 because it has suffered from a prolonged decrease in precipitation for more than 12 years [54, 12, 10].

123 To calculate the drought indices, first we must calculate the accumulation of the variable. In this case, for
124 generalization purposes, we will use V , referring to P , *AED*, D , *NDVI*, and *SM* (Table 1). We cumulated
125 each V over the time series of n values, and for the time scales s :

$$A_{si} = \sum_{i=n-s-i+2}^{n-i+1} V_i \quad \forall i \geq n - s + 1 \quad (2)$$

126 It corresponds to a moving window (convolution) that sums the variable for s starting for the last month
127 n until the month, which could sum for s months ($n-s+1$). Once the variable is cumulated over time for
128 the scale s , we used a nonparametric approach following [37] to derive the drought indices. Thus, the
129 empirically derived probabilities are obtained through an inverse normal approximation [55]. Then, we

130 used the empirical Tukey plotting position [56] over A_i to derive the $P(A_i)$ probabilities across a period of
131 interest:

$$P(A_i) = \frac{i - 0.33}{n + 0.33} \quad (3)$$

132 The drought indices *SPI*, *SPEI*, *EDDI*, *zcSM*, and *zcNDVI* are obtained following the inverse normal
133 approximation:

$$DI(A_i) = W - \frac{C_0 + C_1 \cdot W + c_2 \cdot W^2}{1 + d_1 \cdot W + d_2 \cdot W^2 + d_3 \cdot W^3} \quad (4)$$

134 DI is referring to the drought index calculated for the variable V . The values for the constats are:
135 $C_0 = 2.515517$, $C_1 = 0.802853$, $C_2 = 0.010328$, $d_1 = 1.432788$, $d_2 = 0.189269$, and $d_3 = 0.001308$. For
136 $P(A_i) \leq 0.5$, $W = \sqrt{-2 \cdot \ln(P(A_i))}$, and for $P(A_i) > 0.5$, replace $P(A_i)$ with $1 - P(A_i)$ and reverse the sign
137 of $DI(A_i)$.

138 3.4. Trend of drought indices for water demand and supply, soil moisture, and vegetation productivity

139 To estimate if there are significant positive or negative trends for the drought indices, we used the non-
140 parametric test of Mann-Kendall [57]. To determine the magnitude of the trend, we used Sen's slope [58].
141 One of the advantages of applying this methodology is that the Sen's slope is not affected by outliers as
142 regular regression does. We applied both to the five indices at the six time scales from 1981 to 2023 and
143 indices SPI, EDDI, SPEI, and zcSM, and from 2000 to 2023 in the case of zcNDVI.

144 [59] made a global analysis of the drought's severity trend using SPI, SPEI, and the Standardized Evap-
145 otranspiration Deficit Index (SEDI; [60]) to evaluate AED. They indicate that the increase in hydrological
146 drought has been due to anthropogenic effects rather than climate change. This is because the global in-
147 crease in AED does not explain the change in the spatial pattern of hydrological drought. Also, they state
148 that "*the increase in hydrological droughts has been primarily observed in regions with high water demand*
149 *and land cover change*". We will contrast this hypothesis with what is occurring in Chile. To achieve this,
150 we will use the landcover class type that remain more than 80% of types for 2001-2022, and use this as a
151 mask, where there are low changes, to evaluate the trend on zcNDVI.

152 3.5. LULC change for 2001-2022 and its relation with water supply and demand, and soil moisture

153 To analyze the LULCC, we use the IGBP scheme from the MCD12Q1 collection 6.1 from MODIS. This
154 product has a yearly frequency from 2011 to 2022. The IGBP defines 17 classes; from these, we regrouped
155 into ten macroclasses for forest, schrublands, savannas, grasslands, wetlands, croplands, urban, snow and ice,
156 barren, and water bodies. Then, we calculated the surface occupied per landcover class into each macrozone
157 ("Norte Grande" to "Austral") per year. To determine the trend of change we used the Sen' slope [58] over
158 the surface per year.

159 We calculated a raster mask considering the classes that remains more than 80% of years (2001-2022), which
160 allow us to identify the areas with no landcover change for the macroclasses. Figure 2 shows the summary
161 of proportion of surface per landcover class and macrozone, derived from the mask over continental Chile.

162 We will explore if the trend in landcover classess is associated to trend of the drought indices. For this
163 we will use the regularizations techniques of Lasso [61] and Ridge regression [62]. Also, we will test random
164 forest for this purpose [63].

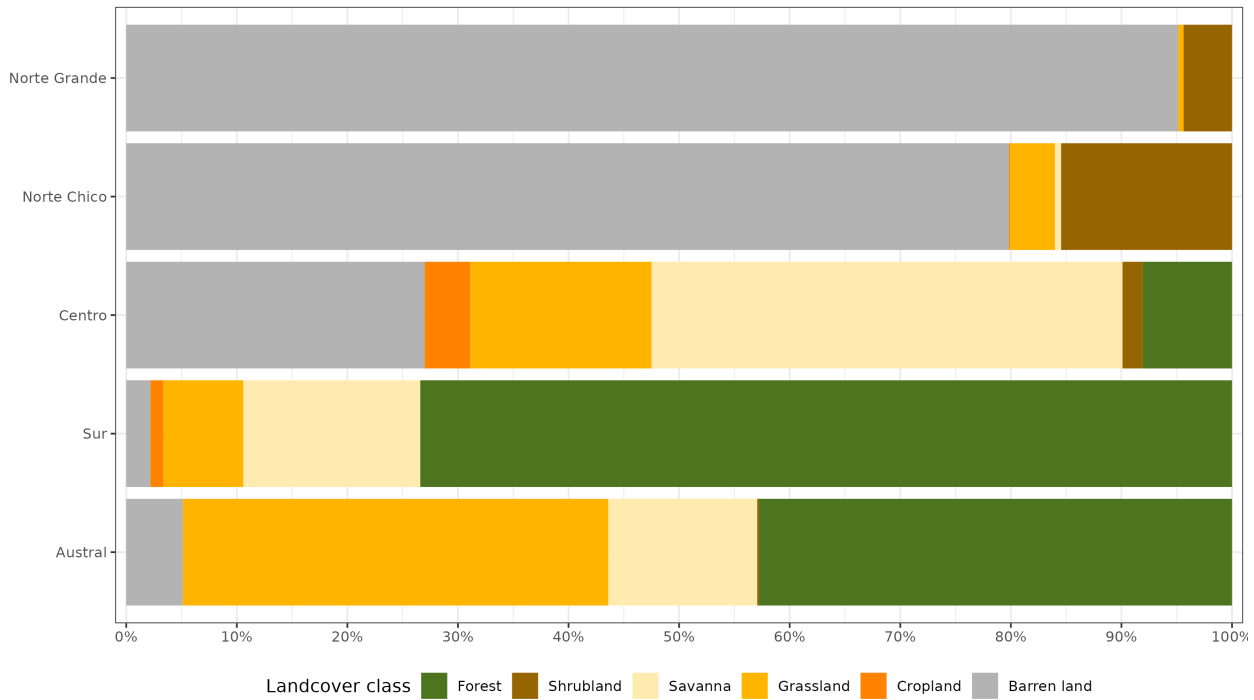


Figure 2: Proportion of land cover class from the persistent land cover for 2001-2022 (>80%) per macrozone

165 3.6. Impact for water supply and demand, and soil moisture in vegetation productivity within landcover types

166 The aim of this section is to analyze the drought indices of water demand and supply and soil moisture
 167 against vegetation to address: i) if short- or long-term time scales are most important in impacting vegetation
 168 through Chile; and ii) the strength of the correlation for the variable and the time scale. Then, we will
 169 summarize for each landcover class and macrozone. Thus, we will be able to advance in understanding how
 170 climate is affecting vegetation, considering the impact on the five macroclasses: forest, cropland, grassland,
 171 savanna, and shrubland.

172 To assess how water demand and supply and soil moisture are related to vegetation productivity (zcNDVI),
 173 we analyze the linear correlation between the indices SPI, SPEI, EDDI, and zcSM for 1, 3, 6, 12, 24, and 36-
 174 month time scales against zcNDVI. We followed a similar approach to that used by [64] when using the SPI
 175 for meteorological drought against the cumulative FAPAR (Fraction of Absorbed Photosynthetically Active
 176 Radiation) as a proxy for vegetation productivity. We made a pixel-to-pixel linear correlation analysis per
 177 index. First, we calculate the Pearson coefficient of correlation for the six time scales and let the time scale
 178 that reaches the maximum correlation be significant ($p < 0.05$). Then, we extracted the Pearson correlation
 179 value corresponding to the time scales that reached the maximum value. Thus, we derived two raster maps
 180 per index, the first with the time scales and the second with the correlation value.

181 3.7. Validation of ERA5-Land variables

182 4. Results

183 4.1. Trend of drought indices for water demand/supply, soil moisture, and vegetation productivity

184 Regarding vegetation productivity, there is a negative trend on zcNDVI in the central part of the country
 185 (“norte chico” and “zona central”) (Figure 3). Indicating either a reduction of vegetation surface, biomass,
 186 or status. It reached its lowest values during the year 2020, mostly on the “zona central.” There are other
 187 negative trends in small areas in “norte grande” and “zona asutral.”

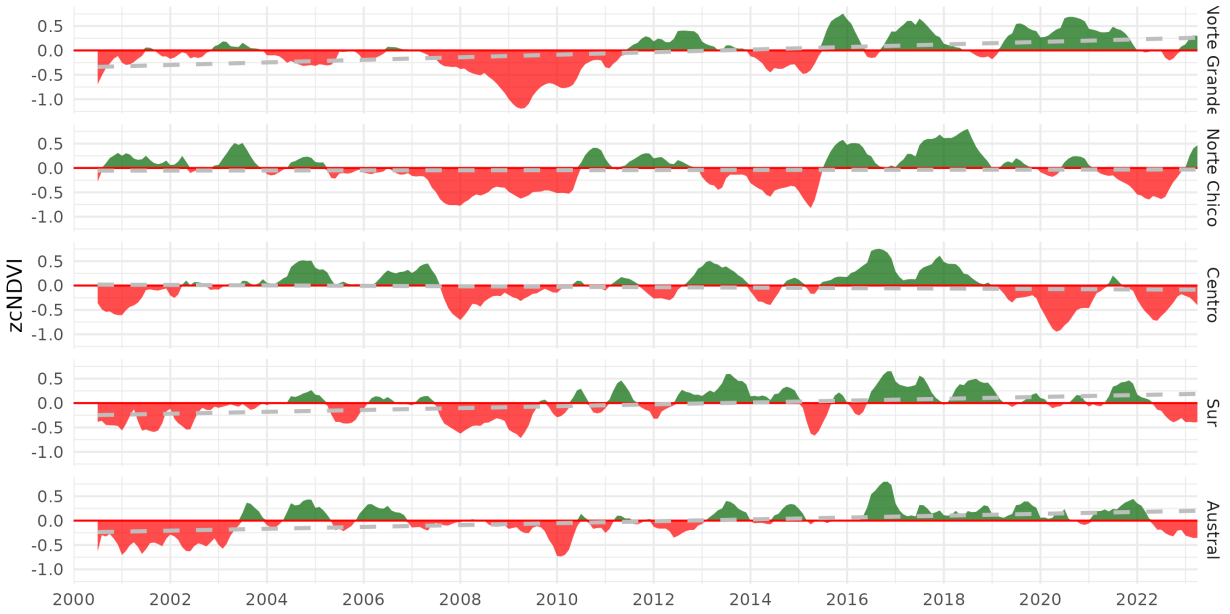


Figure 3: (a) Map of the linear trend of the index zcNDVI-6 for 2001–2023. Greener colors indicate a positive trend and an increase in vegetation development; redder colors correspond to a negative trend and a decrease in vegetation development. (b) Temporal variation of zcNDVI-6 aggregated at macrozone level within continental Chile. Each horizontal panel corresponds to a macrozone from ‘norte grande’ to ‘zona austral’.

188 Analyzing the water supply in the macrozones “norte chico,” “central,” and “sur,” the SPI shows a decreasing
 189 trend that increases at longer time scales due to the prolonged reduction in precipitation. It reaches a
 190 trend of -0.056 (z-score) per decade (Figure 4) for time scales of 36 months. In the case of water demand, we
 191 analyze the EDDI. It shows a positive trend, caused by an increase in AED. The trend on EDDI reaches a
 192 maximum of 0.053 per decade in the macrozones “norte grande” and “norte chico” (Figure 5). The behavior
 193 is similar to SPI, having close trends with opposite signs. Nevertheless, the spatial patterns are different.
 194 The maximum trend for SPI-36 is in “norte chico” and “zona central.” For EDDI-36, the maximum trend
 195 is from “northe grande” to “zona central.”

196 The correlation between zcNDVI-6 and drought indices shows that time scales higher than six months
 197 are predominant over continental Chile in explaining vegetation variability (Figure 6). Pearson correlations
 198 between 0.6 and 0.9 are concentrated in the “norte chico” and “zona central” for SPI and SPEI. Soil moisture
 199 reached a correlation of 0.6–0.9 that extended north and south with respect to SPI.

200 *4.2. Impact for water supply and demand, and soil moisture in vegetation productivity*

201 *4.3. LULC change for 2001-2022 and its relation with water supply and demand, and soil moisture*

202 *4.4. Total water storage (TWS) and drought indices*

203 *4.5. Validation of ERA5-Land variables*

204 **5. Discussion**

205 **6. Conclusion**

206 **References**

- 207 [1] K. Calvin, D. Dasgupta, G. Krinner, A. Mukherji, P. W. Thorne, C. Trisos, J. Romero, P. Aldunce, K. Barrett, G. Blanco,
 208 W. W. Cheung, S. Connors, F. Denton, A. Diougue-Niang, D. Dodman, M. Garschagen, O. Geden, B. Hayward, C. Jones,
 209 F. Jotzo, T. Krug, R. Lasco, Y.-Y. Lee, V. Masson-Delmotte, M. Meinshausen, K. Mintenbeck, A. Mokssit, F. E. Otto,
 210 M. Pathak, A. Pirani, E. Poloczanska, H.-O. Pörtner, A. Revi, D. C. Roberts, J. Roy, A. C. Ruane, J. Skea, P. R.

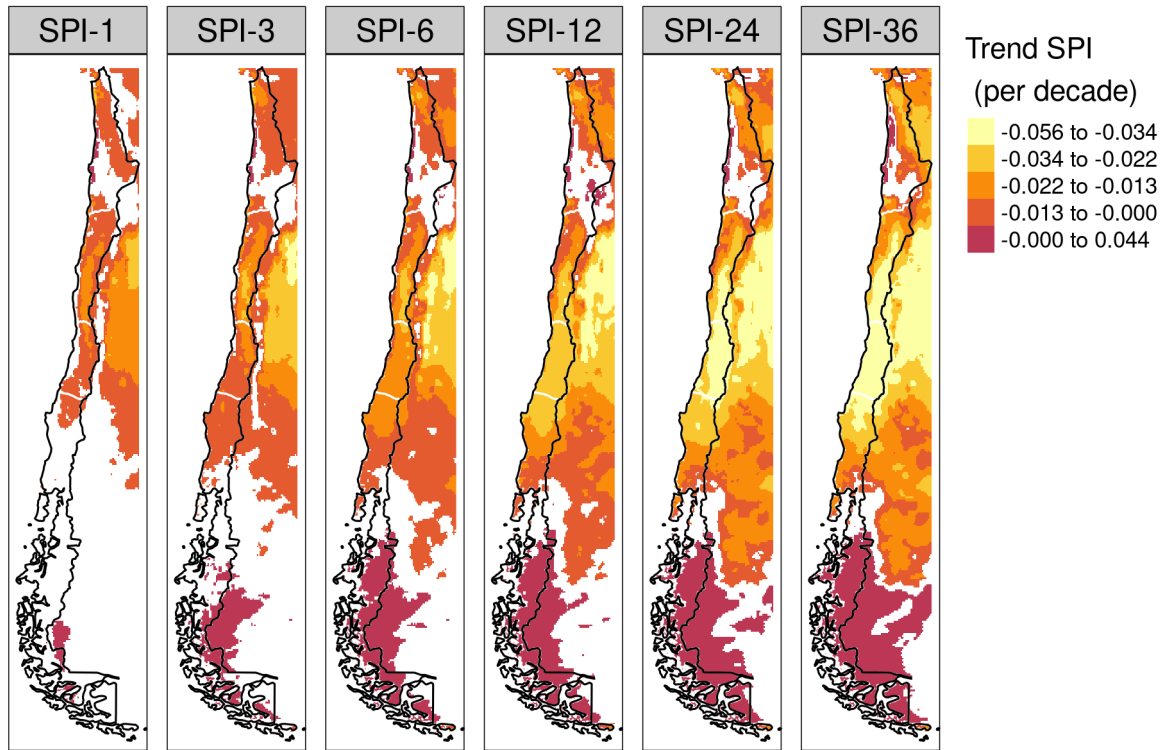


Figure 4: Linear trend of the SPI at time scales of 1, 3, 6, 12, 24, and 36 months for 1981-2023

Table 2: Value of linear change trend next to time-series plot of surface, per landcover class (IGBP MCD12Q1.006) for 2001-2019 through Central Chile. Red dots on the plots indicate the maximum and minimum surface

zone	Trend of change [$\text{km}^2 \text{year}^{-1}$]													
	Forest		Cropland		Grassland		Savanna		Shrubland		Barren land			
	x	y	x	y	x	y	x	y	x	y	x	y		
Norte Grande							0.0				0.0			
Norte Chico							0.0		-70.0		0.0		111.2	
Centro	0.0		-22.4		83.2		-136.2		146.0		22.9			
Sur	396.6		37.8		0.0		-318.8						0.0	
Austral	0.0				0.0		172.1		-36.9		-93.2			

211 Shukla, R. Slade, A. Slangen, Y. Sokona, A. A. Sörensson, M. Tignor, D. Van Vuuren, Y.-M. Wei, H. Winkler, P. Zhai,
212 Z. Zommers, J.-C. Hourcade, F. X. Johnson, S. Pachauri, N. P. Simpson, C. Singh, A. Thomas, E. Totin, P. Arias,
213 M. Bustamante, I. Elgizouli, G. Flato, M. Howden, C. Méndez-Vallejo, J. J. Pereira, R. Pichs-Madruga, S. K. Rose,
214 Y. Saheb, R. Sánchez Rodríguez, D. Ürge Vorsatz, C. Xiao, N. Yassa, A. Alegria, K. Armour, B. Bednar-Friedl, K. Blok,
215 G. Cissé, F. Dentener, S. Eriksen, E. Fischer, G. Garner, C. Guijarch, M. Haasnoot, G. Hansen, M. Hauser, E. Hawkins,
216 T. Hermans, R. Kopp, N. Leprince-Ringuet, J. Lewis, D. Ley, C. Ludden, L. Niamir, Z. Nicholls, S. Some, S. Szopa,
217 B. Trewin, K.-I. Van Der Wijst, G. Winter, M. Witting, A. Birt, M. Ha, J. Romero, J. Kim, E. F. Haites, Y. Jung,
218 R. Stavins, A. Birt, M. Ha, D. J. A. Orendain, L. Ignon, S. Park, Y. Park, A. Reisinger, D. Cammarano, A. Fischlin,
219 J. S. Fuglestvedt, G. Hansen, C. Ludden, V. Masson-Delmotte, J. R. Matthews, K. Mintenbeck, A. Pirani, E. Poloczanska,
220 N. Leprince-Ringuet, C. Péan, [IPCC, 2023: Climate Change 2023: Synthesis Report. Contribution of Working Groups I, II and III to the Sixth Assessment Report of the Intergovernmental Panel on Climate Change \[Core Writing Team, H. Lee and J. Romero \(eds.\)\]. IPCC, Geneva, Switzerland.](#), Tech. rep., Intergovernmental Panel on Climate Change (IPCC) (Jul.
221 2023).
222 URL <https://www.ipcc.ch/report/ar6/syr/>

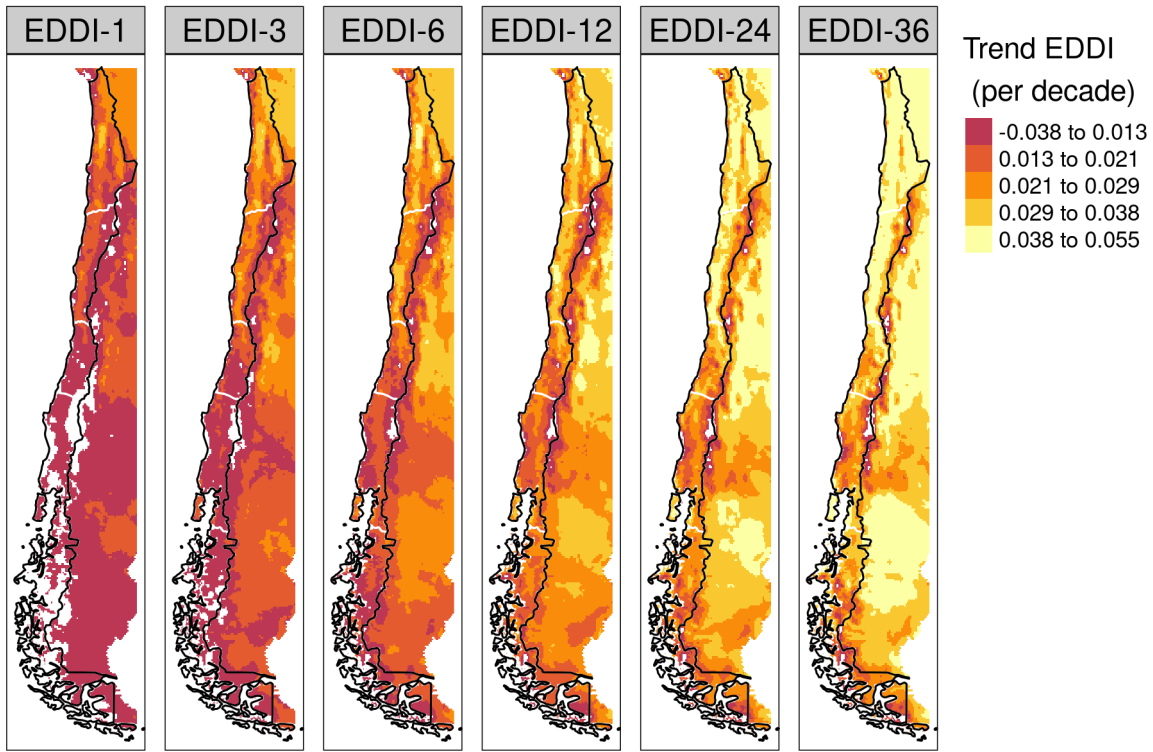


Figure 5: Linear trend of the EDDI at time scales of 1, 3, 6, 12, 24, and 36 months for 1981-2023

Table 3

macro	Forest				Cropland				Grassland				Savanna				Shrubland			
	eddi	spi	spei	zcsm	eddi	spi	spei	zcsm	eddi	spi	spei	zcsm	eddi	spi	spei	zcsm	eddi	spi	spei	zcsm
norte grande									36	36	36	12	36	36	36	24	36	12	36	12
norte chico					36	36	12	12	36	36	24	12	36	24	24	12	36	36	24	12
centro	36	36	12	6	12	12	6	6	12	12	12	36	12	12	12	36	24	24	12	
sur	36				6	6	6	6	6	6	6	12	6	6	6	6	6	12	12	24
austral	6	6				6	12	12	12	6	12	12	6	6	12					
r-squared	 0.2 0.4 0.6																			

- [2] IPCC, [Climate Change 2013: The Physical Science Basis. Contribution of Working Group I to the Fifth Assessment Report of the Intergovernmental Panel on Climate Change](#), Cambridge University Press, Cambridge, UK; New York, USA, 2013. doi:[10.1017/CBO9781107415324](https://doi.org/10.1017/CBO9781107415324). URL www.climatechange2013.org
- [3] X. a. A. M. a. B. W. a. D. C. a. L. A. a. G. S. a. I. I. a. K. J. a. L. S. a. O. F. a. P. I. a. S. M. a. V.-S. S. a. W. M. a. Z. . M.-D. B. a. V. a. O. Seneviratne, S and Zhang, Weather and Climate Extreme Events in a Changing Climate, Cambridge University Press. In Press., 2021, publication Title: Climate Change 2021: The Physical Science Basis. Contribution of Working Group I to the Sixth Assessment Report of the Intergovernmental Panel on Climate Change.
- [4] S. D. Crasbaw, A. R. Ramirez, S. L. Carter, M. S. Cross, K. R. Hall, D. J. Bathke, J. L. Betancourt, S. Colt, A. E. Cravens, M. S. Dalton, J. B. Dunham, L. E. Hay, M. J. Hayes, J. McEvoy, C. A. McNutt, M. A. Moritz, K. H. Nislow, N. Raheem, T. Sanford, [Defining Ecological Drought for the Twenty-First Century](#), Bulletin of the American Meteorological Society 98 (12) (2017) 2543–2550, publisher: American Meteorological Society. doi:[10.1175/BAMS-D-16-0292.1](https://doi.org/10.1175/BAMS-D-16-0292.1).

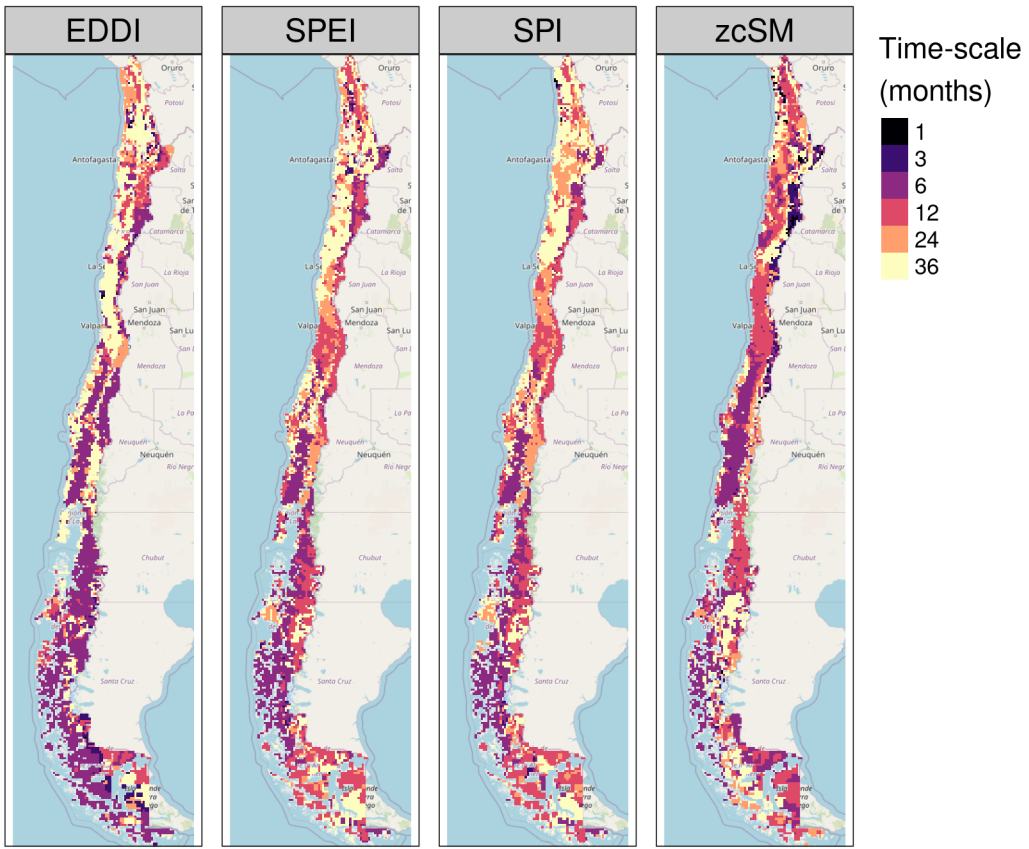


Figure 6: Time scales per drought index that reach the maximum coefficient of determination

- 237 URL <https://journals.ametsoc.org/view/journals/bams/98/12/bams-d-16-0292.1.xml>
- 238 [5] L. Luo, D. Apps, S. Arcand, H. Xu, M. Pan, M. Hoerling, Contribution of temperature and precipitation anomalies to the
239 California drought during 2012–2015, Geophysical Research Letters 44 (7) (2017) 3184–3192. doi:10.1002/2016GL072027.
240 URL <https://agupubs.onlinelibrary.wiley.com/doi/10.1002/2016GL072027>
- 241 [6] D. A. Wilhite, M. H. Glantz, Understanding: The drought phenomenon: The role of definitions, Water International 10 (3)
242 (1985) 111–120. doi:10.1080/02508068508686328.
243 URL <http://dx.doi.org/10.1080/02508068508686328>
- 244 [7] A. F. Van Loon, T. Gleeson, J. Clark, A. I. Van Dijk, K. Stahl, J. Hannaford, G. Di Baldassarre, A. J. Teuling, L. M.
245 Tallaksen, R. Uijlenhoet, D. M. Hannah, J. Sheffield, M. Svoboda, B. Verbeiren, T. Wagener, S. Rangecroft, N. Wanders,
246 H. A. Van Lanen, Drought in the Anthropocene, Nature Geoscience 9 (2) (2016) 89–91. doi:10.1038/ngeo2646.
- 247 [8] A. AghaKouchak, A. Mirchi, K. Madani, G. Di Baldassarre, A. Nazemi, A. Alborzi, H. Anjileli, M. Azarderakhsh, F. Chi-
248 ang, E. Hassanzadeh, L. S. Huning, I. Mallakpour, A. Martinez, O. Mazdiyashi, H. Moftakhari, H. Norouzi, M. Sadegh,
249 D. Sadeqi, A. F. Van Loon, N. Wanders, Anthropogenic Drought: Definition, Challenges, and Opportunities, Reviews of
250 Geophysics 59 (2) (2021) e2019RG000683. doi:10.1029/2019RG000683.
251 URL <https://agupubs.onlinelibrary.wiley.com/doi/10.1029/2019RG000683>
- 252 [9] I. J. Slette, A. K. Post, M. Awad, T. Even, A. Punzalan, S. Williams, M. D. Smith, A. K. Knapp, How ecologists define
253 drought, and why we should do better, Global Change Biology 25 (10) (2019) 3193–3200. doi:10.1111/gcb.14747.
254 URL <https://onlinelibrary.wiley.com/doi/10.1111/gcb.14747>
- 255 [10] R. Garreaud, C. Alvarez-Garreton, J. Barichivich, J. P. Boisier, D. Christie, M. Galleguillos, C. LeQuesne, J. McPhee,
256 M. Zambrano-Bigiarini, The 2010–2015 mega drought in Central Chile: Impacts on regional hydroclimate and vegetation,
257 Hydrology and Earth System Sciences Discussions 2017 (2017) 1–37. doi:10.5194/hess-2017-191.
258 URL <http://www.hydrol-earth-syst-sci-discuss.net/hess-2017-191/>
- 259 [11] F. Zambrano, Four decades of satellite data for agricultural drought monitoring throughout the growing season in Central
260 Chile, in: R. M. Vijay P. Singh Deepak Jhajharia, R. Kumar (Eds.), Integrated Drought Management, Two Volume Set,
261 CRC Press, 2023, p. 28.
- 262 [12] J. P. Boisier, C. Alvarez-Garreton, R. R. Cordero, A. Damiani, L. Gallardo, R. D. Garreaud, F. Lambert, C. Ramallo,
263 M. Rojas, R. Rondanelli, Anthropogenic drying in central-southern Chile evidenced by long-term observations and climate

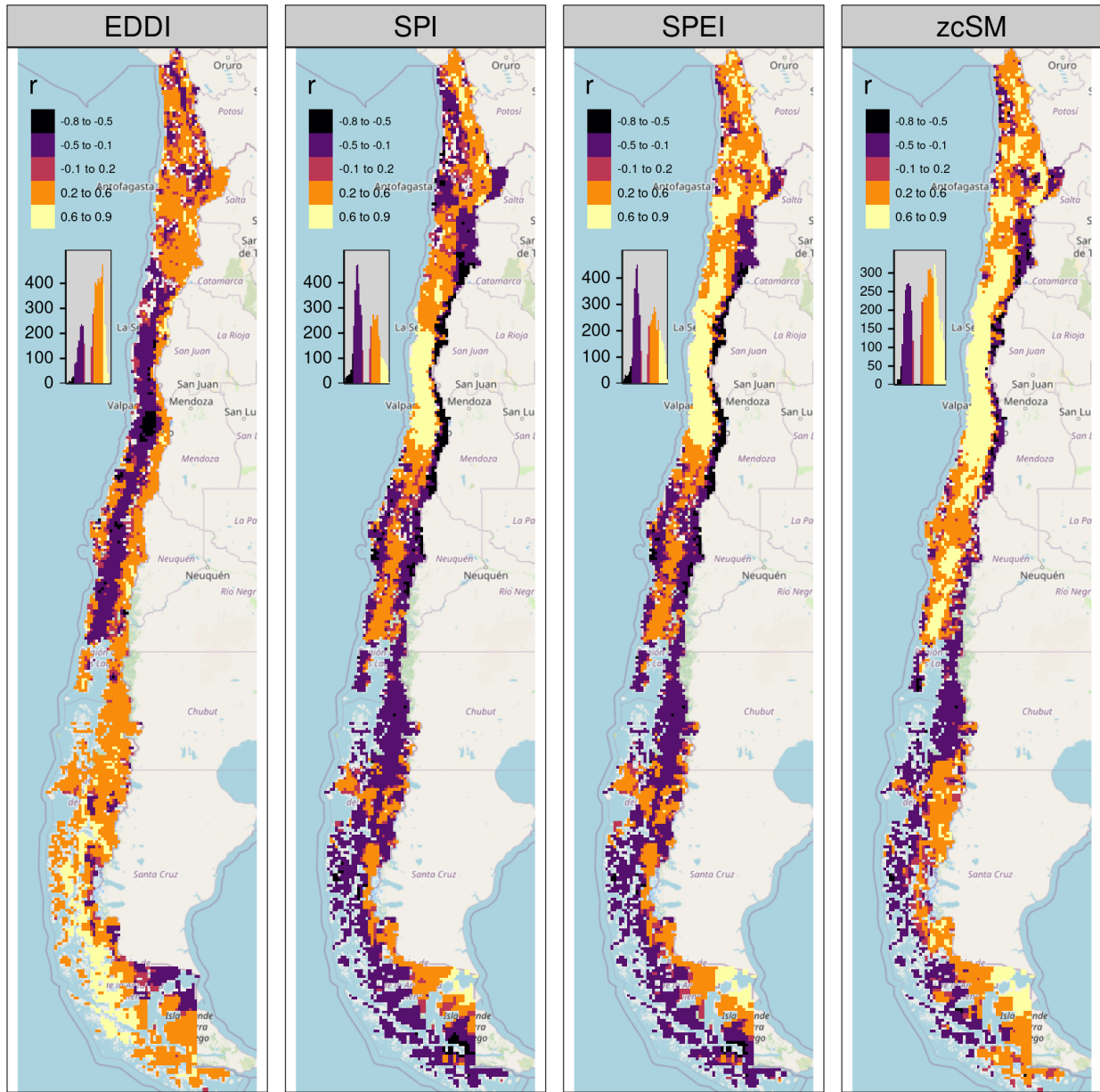


Figure 7: Pearson correlation value for the time scales and drought index that reach the maximum coefficient of determination

- 264 model simulations, *Elementa* 6 (1) (2018) 74. doi:[10.1525/elementa.328](https://doi.org/10.1525/elementa.328).
 265 URL <https://www.elementascience.org/article/10.1525/elementa.328/>
- 266 [13] F. Zambrano, M. Lillo-Saavedra, K. Verbist, O. Lagos, Sixteen years of agricultural drought assessment of the biobío
 267 region in chile using a 250 m resolution vegetation condition index (VCI), *Remote Sensing* 8 (6) (2016) 1–20, publisher:
 268 Multidisciplinary Digital Publishing Institute. doi:[10.3390/rs8060530](https://doi.org/10.3390/rs8060530).
 269 URL <http://www.mdpi.com/2072-4292/8/6/530>
- 270 [14] F. Zambrano, A. Vrieling, A. Nelson, M. Meroni, T. Tadesse, Prediction of drought-induced reduction of agricultural
 271 productivity in Chile from MODIS, rainfall estimates, and climate oscillation indices, *Remote Sensing of Environment* 219
 272 (2018) 15–30, publisher: Elsevier. doi:[10.1016/j.rse.2018.10.006](https://doi.org/10.1016/j.rse.2018.10.006).
 273 URL <https://www.sciencedirect.com/science/article/pii/S0034425718304541>
- 274 [15] A. Miranda, A. Lara, A. Altamirano, C. Di Bella, M. E. González, J. Julio Camarero, Forest browning trends in response
 275 to drought in a highly threatened mediterranean landscape of South America, *Ecological Indicators* 115 (2020) 106401.

- 276 [doi:10.1016/j.ecolind.2020.106401](https://doi.org/10.1016/j.ecolind.2020.106401).
 277 URL <https://linkinghub.elsevier.com/retrieve/pii/S1470160X20303381>
- 278 [16] A. Venegas-González, F. R. Juñent, A. G. Gutiérrez, M. T. Filho, Recent radial growth decline in response to increased
 279 drought conditions in the northernmost Nothofagus populations from South America, *Forest Ecology and Management*
 280 409 (2018) 94–104. [doi:10.1016/j.foreco.2017.11.006](https://doi.org/10.1016/j.foreco.2017.11.006).
 281 URL <https://linkinghub.elsevier.com/retrieve/pii/S0378112717313993>
- 282 [17] R. Urrutia-Jalabert, M. E. González, . González-Reyes, A. Lara, R. Garreaud, Climate variability and forest fires in
 283 central and south-central Chile, *Ecosphere* 9 (4) (2018) e02171. [doi:10.1002/ecs2.2171](https://doi.org/10.1002/ecs2.2171).
 284 URL <https://esajournals.onlinelibrary.wiley.com/doi/10.1002/ecs2.2171>
- 285 [18] I. Fuentes, R. Fuster, D. Avilés, W. Vervoort, Water scarcity in central Chile: the effect of climate and land cover changes
 286 on hydrologic resources, *Hydrological Sciences Journal* 66 (6) (2021) 1028–1044. [doi:10.1080/02626667.2021.1903475](https://doi.org/10.1080/02626667.2021.1903475).
 287 URL <https://www.tandfonline.com/doi/full/10.1080/02626667.2021.1903475>
- 288 [19] C. Alvarez-Garreton, J. P. Boisier, R. Garreaud, J. Seibert, M. Vis, Progressive water deficits during multiyear droughts
 289 in basins with long hydrological memory in Chile, *Hydrology and Earth System Sciences* 25 (1) (2021) 429–446. [doi:10.5194/hess-25-429-2021](https://doi.org/10.5194/hess-25-429-2021).
 290 URL <https://hess.copernicus.org/articles/25/429/2021/>
- 291 [20] F. J. Fernández, F. Vásquez-Lavín, R. D. Ponce, R. Garreaud, F. Hernández, O. Link, F. Zambrano, M. Hanemann, The
 292 economics impacts of long-run droughts: Challenges, gaps, and way forward, *Journal of Environmental Management* 344
 293 (2023) 118726. [doi:10.1016/j.jenvman.2023.118726](https://doi.org/10.1016/j.jenvman.2023.118726).
 294 URL <https://linkinghub.elsevier.com/retrieve/pii/S0301479723015141>
- 295 [21] J. Muñoz-Sabater, E. Dutra, A. Agustí-Panareda, C. Albergel, G. Arduini, G. Balsamo, S. Bousselata, M. Choulga,
 296 S. Harrigan, H. Hersbach, B. Martens, D. G. Miralles, M. Piles, N. J. Rodríguez-Fernández, E. Zsoter, C. Buontempo,
 297 J.-N. Thépaut, ERA5-Land: a state-of-the-art global reanalysis dataset for land applications, *Earth System Science Data*
 298 13 (9) (2021) 4349–4383. [doi:10.5194/essd-13-4349-2021](https://doi.org/10.5194/essd-13-4349-2021).
 299 URL <https://essd.copernicus.org/articles/13/4349/2021/>
- 300 [22] M. Nouri, Drought Assessment Using Gridded Data Sources in Data-Poor Areas with Different Aridity Conditions, *Water
 301 Resources Management* 37 (11) (2023) 4327–4343. [doi:10.1007/s11269-023-03555-4](https://doi.org/10.1007/s11269-023-03555-4).
 302 URL <https://link.springer.com/10.1007/s11269-023-03555-4>
- 303 [23] M. Wang, L. Menzel, S. Jiang, L. Ren, C.-Y. Xu, H. Cui, Evaluation of flash drought under the impact of heat wave events
 304 in southwestern Germany, *Science of The Total Environment* 904 (2023) 166815. [doi:10.1016/j.scitotenv.2023.166815](https://doi.org/10.1016/j.scitotenv.2023.166815).
 305 URL <https://linkinghub.elsevier.com/retrieve/pii/S0048969723054402>
- 306 [24] H. West, N. Quinn, M. Horswell, Remote sensing for drought monitoring \& impact assessment: Progress, past challenges
 307 and future opportunities, *Remote Sensing of Environment* 232, publisher: Elsevier Inc. (Oct. 2019). [doi:10.1016/j.rse.2019.111291](https://doi.org/10.1016/j.rse.2019.111291).
- 308 [25] A. AghaKouchak, A. Farahmand, F. S. Melton, J. Teixeira, M. C. Anderson, B. D. Wardlow, C. R. Hain, Remote
 309 sensing of drought: Progress, challenges and opportunities, *Reviews of Geophysics* 53 (2) (2015) 452–480. [doi:10.1002/2014RG000456](https://doi.org/10.1002/2014RG000456).
 310 URL <http://dx.doi.org/10.1002/2014RG000456>.
- 311 [26] J. M. Paruelo, M. Texeira, L. Staiano, M. Mastrángelo, L. Amdan, F. Gallego, An integrative index of Ecosystem Services
 312 provision based on remotely sensed data, *Ecological Indicators* 71 (2016) 145–154, publisher: Elsevier. [doi:10.1016/J.ECOLIND.2016.06.054](https://doi.org/10.1016/J.ECOLIND.2016.06.054).
 313 URL <https://www.sciencedirect.com/science/article/pii/S1470160X16303843>
- 314 [27] A. Schucknecht, M. Meroni, F. Kayitakire, A. Boureima, A. Schucknecht, M. Meroni, F. Kayitakire, A. Boureima,
 315 Phenology-Based Biomass Estimation to Support Rangeland Management in Semi-Arid Environments, *Remote Sensing*
 316 9 (5) (2017) 463, publisher: Multidisciplinary Digital Publishing Institute. [doi:10.3390/rs9050463](https://doi.org/10.3390/rs9050463).
 317 URL <http://www.mdpi.com/2072-4292/9/5/463>
- 318 [28] H. T. Tran, J. B. Campbell, R. H. Wynne, Y. Shao, S. V. Phan, Drought and Human Impacts on Land Use and Land
 319 Cover Change in a Vietnamese Coastal Area, *Remote Sensing* 2019, Vol. 11, Page 333 11 (3) (2019) 333, publisher:
 320 Multidisciplinary Digital Publishing Institute. [doi:10.3390/RS11030333](https://doi.org/10.3390/RS11030333).
 321 URL <https://www.mdpi.com/2072-4292/11/3/333.htm>
- 322 [29] F. O. Akinyemi, Vegetation Trends, Drought Severity and Land Use-Land Cover Change during the Growing Season
 323 in Semi-Arid Contexts, *Remote Sensing* 2021, Vol. 13, Page 836 13 (5) (2021) 836, publisher: Multidisciplinary Digital
 324 Publishing Institute. [doi:10.3390/RS13050836](https://doi.org/10.3390/RS13050836).
 325 URL <https://www.mdpi.com/2072-4292/13/5/836.htm>
- 326 [30] G. Grekousis, G. Mountarakis, M. Kavouras, An overview of 21 global and 43 regional land-cover mapping products,
 327 *International Journal of Remote Sensing* 36 (21) (2015) 5309–5335. [doi:10.1080/01431161.2015.1093195](https://doi.org/10.1080/01431161.2015.1093195).
 328 URL <https://www.tandfonline.com/doi/full/10.1080/01431161.2015.1093195>
- 329 [31] M. Friedl, D. Sulla-Menashe, MCD12Q1 MODIS/Terra+Aqua Land Cover Type Yearly L3 Global 500m SIN Grid V006
 330 [Data set]. NASA EOSDIS Land Processes DAAC (2019). [doi:10.5067/MODIS/MCD12Q1.006](https://doi.org/10.5067/MODIS/MCD12Q1.006).
- 331 [32] M. Ahmed, M. Sultan, J. Wahr, E. Yan, The use of GRACE data to monitor natural and anthropogenic induced variations
 332 in water availability across Africa, *Earth-Science Reviews* 136 (2014) 289–300, publisher: Elsevier. [doi:10.1016/J.EARSCIREV.2014.05.009](https://doi.org/10.1016/J.EARSCIREV.2014.05.009).
- 333 [33] S. Ma, Q. Wu, J. Wang, S. Zhang, Temporal Evolution of Regional Drought Detected from GRACE TWSA and CCI
 334 SM in Yunnan Province, China, *Remote Sensing* 2017, Vol. 9, Page 1124 9 (11) (2017) 1124, publisher: Multidisciplinary
 335 Digital Publishing Institute. [doi:10.3390/RS9111124](https://doi.org/10.3390/RS9111124).

- 341 URL <https://www.mdpi.com/2072-4292/9/11/1124/htm>
- 342 [34] WMO, M. Svoboda, M. Hayes, D. A. Wood, **Standardized Precipitation Index User Guide**, WMO, Geneva, 2012, series
343 Title: WMO Publication Title: WMO-No. 1090 © Issue: 1090.
344 URL http://library.wmo.int/opac/index.php?lvl=notice_display&id=13682
- 345 [35] T. B. McKee, N. J. Doesken, J. Kleist, The relationship of drought frequency and duration to time scales. In: Proceedings
346 of the Ninth Conference on Applied Climatology., American Meteorological Society (Boston) (1993) 179–184.
- 347 [36] S. M. Vicente-Serrano, S. Beguería, J. I. López-Moreno, **A multiscalar drought index sensitive to global warming: The stan-**
348 **dardized precipitation evapotranspiration index**, Journal of Climate 23 (7) (2010) 1696–1718. doi:[10.1175/2009JCLI2909.1](https://doi.org/10.1175/2009JCLI2909.1)
349
350 URL <http://dx.doi.org/10.1175/2009JCLI2909.1>
- 351 [37] M. T. Hobbins, A. Wood, D. J. McEvoy, J. L. Huntington, C. Morton, M. Anderson, C. Hain, **The Evaporative Demand**
352 **Drought Index. Part I: Linking Drought Evolution to Variations in Evaporative Demand**, Journal of Hydrometeorology
353 17 (6) (2016) 1745–1761. doi:[10.1175/JHM-D-15-0121.1](https://doi.org/10.1175/JHM-D-15-0121.1)
354 URL <http://journals.ametsoc.org/doi/10.1175/JHM-D-15-0121.1>
- 355 [38] D. J. McEvoy, J. L. Huntington, M. T. Hobbins, A. Wood, C. Morton, M. Anderson, C. Hain, **The Evaporative Demand**
356 **Drought Index. Part II: CONUS-Wide Assessment against Common Drought Indicators**, Journal of Hydrometeorology
357 17 (6) (2016) 1763–1779. doi:[10.1175/JHM-D-15-0122.1](https://doi.org/10.1175/JHM-D-15-0122.1)
358 URL <http://journals.ametsoc.org/doi/10.1175/JHM-D-15-0122.1>
- 359 [39] B. Narasimhan, R. Srinivasan, Development and evaluation of Soil Moisture Deficit Index (SMDI) and Evapotranspiration
360 Deficit Index (ETDI) for agricultural drought monitoring, Agricultural and Forest Meteorology 133 (1-4) (2005) 69–88.
361 doi:[10.1016/j.agrformet.2005.07.012](https://doi.org/10.1016/j.agrformet.2005.07.012)
362 URL <https://linkinghub.elsevier.com/retrieve/pii/S0168192305001565>
- 363 [40] A. G. S. S. Souza, A. Ribeiro Neto, L. L. D. Souza, **Soil moisture-based index for agricultural drought assessment: SMADI**
364 **application in Pernambuco State-Brazil**, Remote Sensing of Environment 252 (2021) 112124. doi:[10.1016/j.rse.2020.112124](https://doi.org/10.1016/j.rse.2020.112124).
365 URL <https://linkinghub.elsevier.com/retrieve/pii/S0034425720304971>
- 366 [41] F. N. Kogan, Application of vegetation index and brightness temperature for drought detection, Advances in Space
367 Research 15 (11) (1995) 91–100. doi:[10.1016/0273-1177\(95\)00079-T](https://doi.org/10.1016/0273-1177(95)00079-T)
- 368 [42] A. Cui, J. Li, Q. Zhou, R. Zhu, H. Liu, G. Wu, Q. Li, **Use of a multiscalar GRACE-based standardized terrestrial water**
369 **storage index for assessing global hydrological droughts**, Journal of Hydrology 603 (2021) 126871. doi:[10.1016/j.jhydrol.2021.126871](https://doi.org/10.1016/j.jhydrol.2021.126871).
370 URL <https://linkinghub.elsevier.com/retrieve/pii/S0022169421009215>
- 371 [43] P. Aceituno, J. P. Boisier, R. Garreaud, R. Rondanelli, J. A. Ruttlant, **Climate and Weather in Chile**, in: B. Fernández,
372 J. Gironás (Eds.), Water Resources of Chile, Vol. 8, Springer International Publishing, Cham, 2021, pp. 7–29.
373 URL https://link.springer.com/10.1007/978-3-030-56901-3_2
- 374 [44] R. D. Garreaud, **The Andes climate and weather**, Advances in Geosciences 22 (2009) 3–11. doi:[10.5194/adgeo-22-3-2009](https://doi.org/10.5194/adgeo-22-3-2009).
375 URL <https://adgeo.copernicus.org/articles/22/3/2009/>
- 376 [45] H. E. Beck, T. R. McVicar, N. Vergopolan, A. Berg, N. J. Lutsko, A. Dufour, Z. Zeng, X. Jiang, A. I. J. M. van Dijk, D. G.
377 Miralles, **High-resolution (1 km) Köppen-Geiger maps for 1901–2099 based on constrained CMIP6 projections**, Scientific
378 Data 10 (1) (Oct. 2023). doi:[10.1038/s41597-023-02549-6](https://doi.org/10.1038/s41597-023-02549-6).
379 URL <https://dx.doi.org/10.1038/s41597-023-02549-6>
- 380 [46] K. Didan, MOD13Q1 MODIS/Terra Vegetation Indices 16-Day L3 Global 250m SIN Grid V006, Tech. rep., NASA EOSDIS
381 Land Processes DAAC (2015). doi:[http://dx.doi.org/10.5067/MODIS/MOD13Q1.006](https://dx.doi.org/10.5067/MODIS/MOD13Q1.006).
- 382 [47] R Core Team, **R: A Language and Environment for Statistical Computing**, R Foundation for Statistical Computing,
383 Vienna, Austria, 2023.
384 URL <https://www.R-project.org/>
- 385 [48] K. Hufkens, R. Stauffer, E. Campitelli, **The ecwmfr package: an interface to ECMWF API endpoints** (2019).
386 URL <https://bluegreen-labs.github.io/ecmwfr/>
- 387 [49] R. J. Hijmans, **terra: Spatial Data Analysis**, 2023.
388 URL <https://CRAN.R-project.org/package=terra>
- 389 [50] E. Pebesma, R. Bivand, **Spatial Data Science: With applications in R**, Chapman and Hall/CRC, London, 2023.
390 URL <https://r-spatial.org/book/>
- 391 [51] E. Pebesma, **Simple Features for R: Standardized Support for Spatial Vector Data**, The R Journal 10 (1) (2018) 439–446.
392 doi:[10.32614/RJ-2018-009](https://doi.org/10.32614/RJ-2018-009).
393 URL <https://doi.org/10.32614/RJ-2018-009>
- 394 [52] S. Beguería, S. M. Vicente-Serrano, **SPEI: Calculation of the Standardized Precipitation-Evapotranspiration Index**, 2023.
395 URL <https://CRAN.R-project.org/package=SPEI>
- 396 [53] G. H. Hargreaves, **Defining and Using Reference Evapotranspiration**, Journal of Irrigation and Drainage Engineering
397 120 (6) (1994) 1132–1139. doi:[10.1061/\(ASCE\)0733-9437\(1994\)120:6\(1132\)](https://doi.org/10.1061/(ASCE)0733-9437(1994)120:6(1132)).
398 URL <https://ascelibrary.org/doi/10.1061/%28ASCE%290733-9437%281994%29120%3A6%281132%29>
- 399 [54] R. D. Garreaud, J. P. Boisier, R. Rondanelli, A. Montecinos, H. H. Sepúlveda, D. Veloso-Aguila, **The Central Chile**
400 **Mega Drought (2010–2018): A climate dynamics perspective**, International Journal of Climatology 40 (1) (2020) 421–439.
401 doi:[10.1002/joc.6219](https://doi.org/10.1002/joc.6219).
402 URL <https://rmets.onlinelibrary.wiley.com/doi/10.1002/joc.6219>
- 403 [55] M. Abramowitz, I. A. Stegun, **Handbook of mathematical functions with formulas, graphs, and mathematical tables**,

- 406 Vol. 55, US Government printing office, 1968.
- 407 [56] D. S. Wilks, Empirical distributions and exploratory data analysis, Statistical Methods in the Atmospheric Sciences 100
 408 (2011).
- 409 [57] M. Kendall, Rank correlation methods (4th ed, 2d impression). Griffin, 1975.
- 410 [58] P. K. Sen, [Estimates of the Regression Coefficient Based on Kendall's Tau](#), Journal of the American Statistical Association
 411 63 (324) (1968) 1379–1389. [doi:10.1080/01621459.1968.10480934](#).
- 412 URL <http://www.tandfonline.com/doi/abs/10.1080/01621459.1968.10480934>
- 413 [59] S. M. Vicente-Serrano, D. Peña-Angulo, S. Beguería, F. Domínguez-Castro, M. Tomás-Burguera, I. Noguera, L. Gimeno-
 414 Sotelo, A. El Kenawy, [Global drought trends and future projections](#), Philosophical Transactions of the Royal Society A:
 415 Mathematical, Physical and Engineering Sciences 380 (2238) (2022) 20210285. [doi:10.1098/rsta.2021.0285](#).
 416 URL <https://royalsocietypublishing.org/doi/10.1098/rsta.2021.0285>
- 417 [60] S. M. Vicente-Serrano, D. G. Miralles, F. Domínguez-Castro, C. Azorin-Molina, A. El Kenawy, T. R. McVicar, M. Tomás-
 418 Burguera, S. Beguería, M. Maneta, M. Peña-Gallardo, [Global Assessment of the Standardized Evapotranspiration Deficit
 419 Index \(SEDI\) for Drought Analysis and Monitoring](#), Journal of Climate 31 (14) (2018) 5371–5393. [doi:10.1175/JCLI-D-
 420 17-0775.1](#).
 421 URL <https://journals.ametsoc.org/doi/10.1175/JCLI-D-17-0775.1>
- 422 [61] R. Tibshirani, J. Bien, J. Friedman, T. Hastie, N. Simon, J. Taylor, R. J. Tibshirani, [Strong rules for discarding predictors
 423 in lasso-type problems](#) (Nov. 2010).
 424 URL <http://arxiv.org/abs/1011.2234>
- 425 [62] A. E. Hoerl, R. W. Kennard, [Ridge Regression: Biased Estimation for Nonorthogonal Problems](#), Technometrics 12 (1)
 426 (1970) 55–67. [doi:10.1080/00401706.1970.10488634](#).
 427 URL <http://www.tandfonline.com/doi/abs/10.1080/00401706.1970.10488634>
- 428 [63] T. K. Ho, Random decision forests, in: Proceedings of 3rd international conference on document analysis and recognition,
 429 Vol. 1, IEEE, 1995, pp. 278–282.
- 430 [64] M. Meroni, F. Rembold, D. Fasbender, A. Vrieling, [Evaluation of the Standardized Precipitation Index as an early
 431 predictor of seasonal vegetation production anomalies in the Sahel](#), Remote Sensing Letters 8 (4) (2017) 301–310. [doi:
 432 10.1080/2150704X.2016.1264020](#).
 433 URL <https://www.tandfonline.com/doi/full/10.1080/2150704X.2016.1264020>